Transient surface tension in miscible liquids

Laurent Lacaze,[1,2] Patrick Guenoun,[2,*] Daniel Beysens,[1,3] Michel Delsanti,[2] Philippe Petitjeans,[1] and Pascal Kurowski[1]

[1]*Laboratoire de Physique et Mécanique des Milieux Hétérogènes (PMMH), Ecole Supérieure de Physique et de Chimie Industrielles (ESPCI), 10 rue Vauquelin, 75231 Paris Cedex 5, France*

[2]*IRAMIS, LIONS, UMR SIS2M 3299 CEA-CNRS, CEA-Saclay, F-91191 Gif-Sur-Yvette Cedex, France*

[3]*CEA, INAC, Service des Basses Températures, F-38042 Grenoble, France*

Evidence of the existence of a transient surface tension between two miscible fluid phases is given. This is done by making use of a density matched free of gravity perturbations, binary liquid of isobutyric acid and water, which presents a miscibility gap and is studied by light scattering. The experiment is performed very near the critical point of the binary liquid, where the diffusion of phases is extremely slow. The surface tension is deduced from the evolution of the structure factor obtained from low angle light scattering. The latter evolution is successfully analyzed in terms of a local equilibrium diffusive approach that makes explicit how the surface tension decreases with time.

PACS number(s): 68.05.−n, 05.60.Cd, 64.70.Ja

I. INTRODUCTION

When a drop of wine is gently immersed in a glass of water from the tip of a pen, after unavoidable initial hydrodynamics and buoyancy effects, some experiments show that the drop, before dissolving away, can retain for a while a ringlike compact shape [1]. It looks like as if a nonzero surface tension between both phases, nevertheless completely miscible, could persist for some time. From a mechanical point of view, surface tension can be calculated as an integral of unbalanced tangential stresses over the interface thickness [2,3]. It is thus of no surprise that, within the assumption of temporal and local equilibrium, such a tension can be ascribed to an interface between two miscible fluids [4] and assumes a nonzero value. This was first considered by Korteweg [5], who introduced the so-called Korteweg stresses due to concentration inhomogeneities.

The determination of such a transient surface tension should play an important role in numerous applications of fluid mechanics, where mixing of two fluids needs to be mastered down to small scales (microfluidics). A transient surface tension between two miscible phases appears also as a necessary input in the numerical simulations of miscible fluids when modeling Rayleigh-Taylor instabilities [6] or Hele-Shaw flows [7].

A number of attempts to measure a transient surface tension have been carried out so far by different techniques. Following a pioneering study on geophysical fluids by Mungall [8], a couple of experimental studies have used the rotating drop method in order to put directly into contact two fluids and measure the surface tension [1]. Such a surface tension determination necessitates a precise knowledge of the evolution of the phase densities, which is not always available [9–12]. Moreover, the method of analysis of the drop profile is often delicate since the standard conditions of a single elongated cylinder are not always met. Other attempts dealt with measurements of the light scattered by a

gravity-pinned planar interface between partially miscible liquids, suddenly quenched from the two-phase region to the one-phase region [13,14]. The step in temperature made in both cases was of several tenths of degrees across the critical point. This leads to a temporal evolution that is mostly not isothermal since the surface tension varies strongly with temperature when approaching the critical point. Moreover, the origin of the scattered light can be attributed to both thermally activated capillary waves (giving access to surface tension) and bulk nonequilibrium concentration fluctuations (due to the widening interface) [14]. In the one-phase region, these latter bulk fluctuations tend to be dominant over the single interface signal, making the surface signal delicate to detect.

In the experiments presented here, we choose another experimental configuration aimed at reaching a quasi-isothermal behavior and at maximizing the surface signal over the bulk fluctuation signal. We investigate by light-scattering techniques the bulk remixing of a partially miscible binary liquid (isobutyric acid and water, denoted IW) initially in its two-phase region very close to its critical point. In this region, well-known critical slowing down allows precise time-resolved measurements to be performed, and a universal evolution, which follows scaling laws in temperature, can be used with confidence (see, e.g., Chap. 8.5 in [15]). We are then able (i) to precisely locate the time where the system returns to the one-phase region and (ii) to follow a quasi-isothermal behavior for the surface tension relaxation. Our detected signal relies on correlation between multiple interfaces (structure factor) and is dominant over bulk scattering as long as interfaces are sharp enough.

The IW mixture exhibits an upper critical solution temperature. The initial state of the mixture is prepared at a temperature $T > T_c$ (the critical temperature), where the system is homogeneous (one-phase region). Phase separation and subsequent remixing are triggered by two successive thermal quenches, a first quench below T_c, and a second quench above T_c. The quenches are precisely controlled by using a thin sample immersed in a thermostat with temperature control within 0.2 mK. Provided the phase transition time scale is adapted, the initial two-phase state developing

*patrick.guenoun@cea.fr

during the first quench can be described as a set of random interfaces whose evolution is precisely known and driven for long times by surface tension [16]. In addition, the IW mixture exhibits density matching, so that gravity perturbations (buoyancy flows) are absent [17].

Along this first quench below T_c, if no further action was taken, the domains of both phases would grow—thanks to capillary flows—and eventually give rise to two macroscopically well separated phases due to long term gravity sedimentation and wetting forces. Before reaching this final state, the second thermal quench above T_c drives the mixture back to the one-phase region. During all the quenches, light scattering through the sample provides the structure factor of the domains, which is the Fourier transform of the domain correlation function. The evolution of the domains during the first quench is driven by both the mutual diffusion of the species ("demixing") and the domain coalescences, the latter inducing capillary flows. During the second upward quench, mutual diffusion again ("remixing") and possible capillary flows, due to the expected transient surface tension, contribute to the dynamics.

In this paper, we show that capillary flows persist for some time when the mixture is quenched back to the one-phase region, during the second quench. The interfacial tension is then deduced from the persistence of capillary flows and is shown to vanish with time according to a simple diffusion model.

II. EXPERIMENTAL

The IW mixture is used at critical concentration (acid mass fraction of 0.3885) [18]. Its miscibility critical temperature is $T_c \sim 26.5$ °C. This value can appreciably change with the presence of even minute impurity concentrations in the cell. Its experimental determination is thus necessary prior to each experiment. It is obtained within a precision of 0.4 mK from light transmittancy measurements. A parallelepipedic fused-quartz cell of 2 mm inner width with walls of 1 mm thickness is filled with the mixture and placed in a copper oven coupled to a temperature regulation within 0.1 mK (ATNE, France). This temperature control system enables one also to quench up or down the system in temperature. The thermal evolution of the sample is monitored by *in situ* optical measurements through the sample (light transmittancy) by shining a laser beam whose power is low enough (<0.1 mW) so as not to heat the sample. Since the transmitted light intensity varies like $I_t \sim (T - T_c)$ [19], the temperature variation can be then determined in the sample precisely at the beam location and provides the accurate requested determination of T_c. The quench down is limited by the small natural cooling heat flux with a thermal constant of order 20 s. The parameters of the temperature regulation are chosen to minimize the time of quenching up, which is of order 10 s.

The light scattered from the cell is detected at small angles by a charge-coupled device camera. The transfer wave vector is $k = 4\pi n \sin(\theta/2)/\lambda_0$, where λ_0 (633.3 nm) is the laser wavelength in vacuum, $n = 1.3568$ is the mixture refractive index for this wavelength [20], and θ is the scattering angle in the liquid. Details on the small-angle scattering setup can be found in Ref. [21].

A typical double-quench experiment goes as follows. Initially, the mixture is stirred at $T_c + 10$ K, where it homogenizes. Then, temperature is gradually decreased down to temperature T_i at a few mK above T_c. At a time $t = t_I$, the mixture is quenched down to the temperature T_f at a few mK below T_c, where it phase separates. After some time on order of 30–40 s, the mixture is quenched back up at a time $t = t_{II}$ to the initial temperature T_i. The scattered light $I_s(k, t, T)$ is recorded throughout the whole process.

In order to obtain the structure factor $S(k, t, T)$ due to the interfaces, a background contribution $I_b(k, t, T)$ has to be subtracted from the raw signal $I_s(k, t, T)$. This background corresponds to the bulk scattering fluctuations plus the parasitic contributions (cell windows, optics). Its contribution could be estimated from the stationary equilibrium intensity $I_b(k, T_i)$ recorded at the temperature T_i in the one phase region, i.e., $I_b(k, T_i) = I_s(k, T_i)$. However, it was observed that such a treatment does not account for a perfect subtraction at high wave vectors presumably because those fluctuations are nonequilibrium. Actually, during phase separation, the high wave-vector fluctuations are not identical to the Ornstein-Zernike-type fluctuations of the one-phase region but are nonequilibrium fluctuations, which add up to large scale correlations of domains measured by the structure factor. We then chose to model these fluctuations by a simple multiplicative factor $\beta(t)$ since we do not expect these fluctuations to have any structure in the wave-vector range of $S(k, t)$. This factor ensures that $S(k, t)$ goes to zero outside the k window under study, an approximate but reasonable assumption. The factor $\beta(t)$ is such as $I_b(k, t, T) = \beta(t) \times I_s(k, T_i)$. It is determined to obtain $I_s(k, t, T) - \beta(t) I_s(k, T_i) = 0$ for 2.48×10^6 m$^{-1} < k < k_{max}$, where $k_{max}(=2.53 \times 10^6$ m$^{-1})$ is the maximum accessible wave vector of the setup. In order to extract the structure factor after the background subtraction, a normalization is performed: $S(k, t, T) \propto [I_s(k, t, T) - I_b(k, t, T)]/\beta(t)$. An example of such a treatment is given in Fig. 1.

It must be noted that the background subtraction from the scattered light is only useful for assessing the scaling behavior of the structure factor. It is not necessary for the discussion of the evolution of the peak of the structure factor with time.

III. RESULTS

Several double quenches have been carried out. Common features are observed for all of them, and we report here about four double quenches (see Table I). After 30–40 s of separation at T_f, the mixture was quenched back up to T_i. For $T < T_c$, $S(k, t, T)$ is a peak-shaped curve as a function of k. The position of the maximum $S_m(t, T) = S(k = k_m, t, T)$ corresponds to the mean distance $L_m(t) = 2\pi/k_m(t)$ between the growing domains of the separating phases at temperature T. As time increases, the maximum $S_m(t, T)$ increases and $k_m(t, T)$ diminishes, the latter behavior showing the phases coarsening. Relying on scaling assumptions and experiments, a time invariant scaling form $F(x)$ has been proposed (see, e.g., Eq. 8.3.13 in [15]). With $x = k/k_m$, it reads
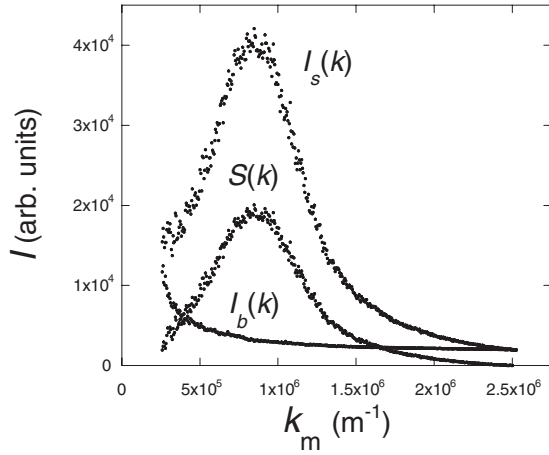
FIG. 1. Structure factor $S(k)$ from the raw scattered intensity [$I_s(k)$, arbitrary units] and the background intensity [$I_b(k)$, arbitrary units] at $t=7.5$ s and for a quench of 5 mK below T_c. $S(k)$ is obtained by subtracting to the raw intensity a background term which is assumed to be homothetic to the one-phase fluctuation background. The background level is adjusted to make $S(k)$ null at the highest wave vector (see text).

$$F(x) = \frac{k_m(t)^3 S(k,t)}{\int k^2 S(k,t) dk}. \tag{1}$$

The integral in Eq. (1) is performed from $k_m/2$ to $2k_m$ and is weakly sensitive to the choice of the integration interval. Such a scaling behavior is shown in Figs. 2(a) and 2(b) for a quench of 5 mK amplitude (set 2 in Table I). In this case, $t_I=-40$ s and $t_{II}=0$ s. Scaling is typically observed from 30 s after the beginning of the first quench below T_c.

For $T > T_c$ $S(k,t,T)$ is still a peak-shaped curve as a function of k and, for some time, coarsening persists as the position of the maximum of the curve, $k_m(t,T)$, keeps decreasing with time. Scaling is preserved until about 20 s after the beginning of the second quench above T_c.

IV. DISCUSSION

A. Evolution below T_c

The evolution of $k_m(t)$ in the two-phase region can be cast into a universal scaling form when expressed with reduced quantities $k_m^*(t)=k_m(t)\xi^-$ and $t^*=t/t_{\xi^-}$ (see, e.g., the introduction of Section 8.5 in [15]). ξ^- is the correlation length of critical fluctuations below T_c. It varies as a function of the distance to T_c as $\xi^-=\xi_0^-\epsilon^{-\nu}$, where $\epsilon=|(T-T_c)/T_c|$ is the reduced temperature and $\nu=0.63$. The nonuniversal amplitude is $\xi_0^-=0.181$ nm for IW [22]. The time t_{ξ^-} is the typical diffusion time of a critical fluctuation. It can be expressed as [15]

$$t_{\xi^-} = \frac{(\xi^-)^2}{D^-}. \tag{2}$$

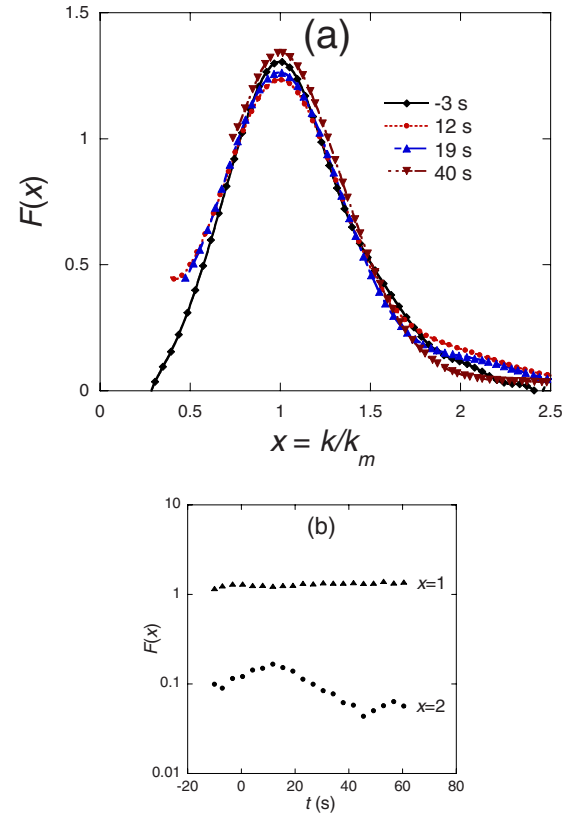Here, D^- is the diffusion constant below T_c, which can be written as

FIG. 2. (Color online) (a) Scaled evolution of the reduced structure factor $F(x)$ after a quench to T_c-5 mK at time $t_I=-40$ s and T_c+5 mK at $t_{II}=0$ s. Scaling is not yet established at $t=-3$ s while it is observed at later times (here are shown $t=12$ and 19 s). Later on it breaks down at $t=40$ s. (b) Evolution of $F(x)$ for two characteristic x values; $x=2$ highlights the breaking of scaling at $t \simeq 20$ s.

$$D^- = \frac{k_B T_c}{6\pi\eta\xi^-}, \tag{3}$$

where η is the shear viscosity, which remains almost constant near T_c and equals 2.9×10^{-3} Pa s for IW [22].

The process of phase separation below T_c can be understood as follows [23]. At early times, just after the mixture is quenched below T_c (time $t^* \approx 1$), domains of both phases nucleate on critical fluctuations ($k_m^* \approx 1$). The concentration and size of domains grow by diffusion, corresponding to the diffusive part of the k_m evolution,

$$k_{m,d}^* \sim t^{*-1/3}. \tag{4}$$

At the same time, the domains coalesce, inducing hydrodynamics flows of capillary origin that speed up the process and correspond to the hydrodynamic component of the k_m evolution. At low Reynolds number, in the viscous limit, this component is proportional to time and corresponds to

$$k_{m,h}^* \sim t^{*-1}. \tag{5}$$

While at early time both diffusion and coalescence contribute to the growth of domains, at late times ($t^* > \sim 10^3$) only coalescence-induced capillary flows dominate the evolution,

TABLE I. Results of the fits to the L_m evolution below and above T_c. The underlined numbers are imposed in the fits. The symbol σ_{fit} is used for both fits of the surface tension in the two-phase region (upper part of the table) and of the prefactor of the transient surface tension in the one-phase region (lower part of the table).

	L_m (m)	Set	$T-T_c$ (mK)	σ (10^{-9} N m^{-1})	t_1 (s)	t_2 (s)	L_0 (10^{-6} m)	σ_{fit}/σ	$l_{i,fit}$ (10^{-6} m)	D (10^{-13} m s^{-2})	$l_i=16\xi^-$ (10^{-6} m)	$l_{i,fit}/l_i$
$T<T_c$	$2.84\times10^{-6}(t-t_1)^{1/3}$ $+8.70\times10^{-2}(\sigma/\eta)(t-t_1)$	1	-3	6.0	-18.9 ± 0.3			0.64 ± 0.15				
		2	-5	11.0	-12.5 ± 0.2			0.36 ± 0.01				
		3	-3	6.0	-28.3 ± 0.4			0.93 ± 0.02				
		4	-3	6.0	-27.0 ± 0.4			0.88 ± 0.03				
$T>T_c$	$L_0+8.70\times10^{-2}\times(\sigma/\eta)(t-t_2)$ $/[1+4\pi D^+(t-t_2)/l_i^2]^{1/2}$	1	$+3$			$\underline{10}$	8.5 ± 0.4	2.2 ± 0.3	7.7 ± 1	1.48	4.08	1.9 ± 0.3
		2	$+5$			$\underline{10}$	8.5 ± 0.3	0.8 ± 0.1	8.9 ± 2	2.04	2.96	3 ± 1
		3	$+4$			$\underline{7}$	11.9 ± 0.07	2.9 ± 1	4.6 ± 0.2	1.77	4.08	1.13 ± 0.05
		4	$+7$			$\underline{5}$	9.3 ± 1.2	1.1 ± 0.5	6.7 ± 3	2.52	4.08	1.64 ± 0.7

i.e., $k_m \approx k_{m,h}$. More precisely, when written in nonscaled variables, Eq. (5) reflects the growth of domains of size $L_{m,h}$ due to capillary instabilities driven by the interfacial tension σ,

$$L_{m,h} = \frac{2\pi}{k_{m,h}} \propto \frac{\sigma}{\eta} t. \quad (6)$$

This dual diffusive and hydrodynamic behavior was described by Furukawa [24], who gave a solution for k_m^* in the form

$$(k_m^* - 1) - [(A^*/B^*)^{1/2}\{\tan^{-1}[k_m^*(B^*/A^*)^{1/2}] \\ - \tan^{-1}[(B^*/A^*)^{1/2}]\}] = B^*t^*, \quad (7)$$

where A^* and B^* are adjustable parameters. For binary liquids [17], $A^* \sim 0.14$ and $B^* \sim 0.022$ are found to reproduce the experimental data.

In the time and temperature range investigated here [20 $< (t-t_I)^* < 500$], an approximation of the above solution [Eq. (7)] reads $L_m^* = 6.785t^{*1/3} + 0.157t^*$, where the coefficients are known within 20% because of the scattering of experimental data. This uncertainty will be taken into account in the fits presented below. Making use of the universal relation [25]

$$\sigma = k_B T/10.4(\xi^-)^2, \quad (8)$$

one obtains in terms of direct-space variables

$$L_m = a(t-t_1)^{1/3} + b\frac{\sigma}{\eta}(t-t_1), \quad (9)$$

with $a = 2.84\times10^{-6}$ m s$^{-1/3}$ and $b = 8.70\times10^{-2}$. The time t_1 takes into account the actual equilibration time of the sample, and the difference with t_I is due to the thermal diffusion in the thermostat and the sample. Note that the present mixture is closely density matched [26] and the effect of gravity on the flows is thus negligible [27]. This means that the evolution during quench I is limited to the range defined as $k_m l_c > 1$, where l_c is the capillary length. During the evolution below T_c the structure factor progressively develops, but the scaling in $F(x)$ is observed typically 30 s after t_I ($t > -10$ s), as shown in Fig. 2. As already noted, this is due to the thermal delay between the fluid and the thermostat and the time needed for thermal gradients to fade away.

The domain evolution is fitted—thanks to Eq. (9) (Fig. 3)—and the best fit is obtained for $a = 2.27\times10^{-6}$ m s$^{-1/3}$, a value within the 20% uncertainty range of the nominal value. Since the exact time delay for reaching the temperature equilibrium in the sample is unknown, we consider the origin of time t_1 and the (temperature-dependent) surface tension as adjustable parameters. The result of the fits are given in Table I, upper line, where the value of σ is obtained by making use of Eq. (8). As expected, the values for t_1 are found to be on the order of -15 s. The surface tension σ_{fit} is found to be somewhat lower than the expected value σ at temperature T_f, the largest discrepancy being found for the deepest quench where the equilibration time is the largest. This can be due to the fact that the fluid has not reached its final equilibrium temperature yet. (The error on σ can also originate from the uncertainty on b.)
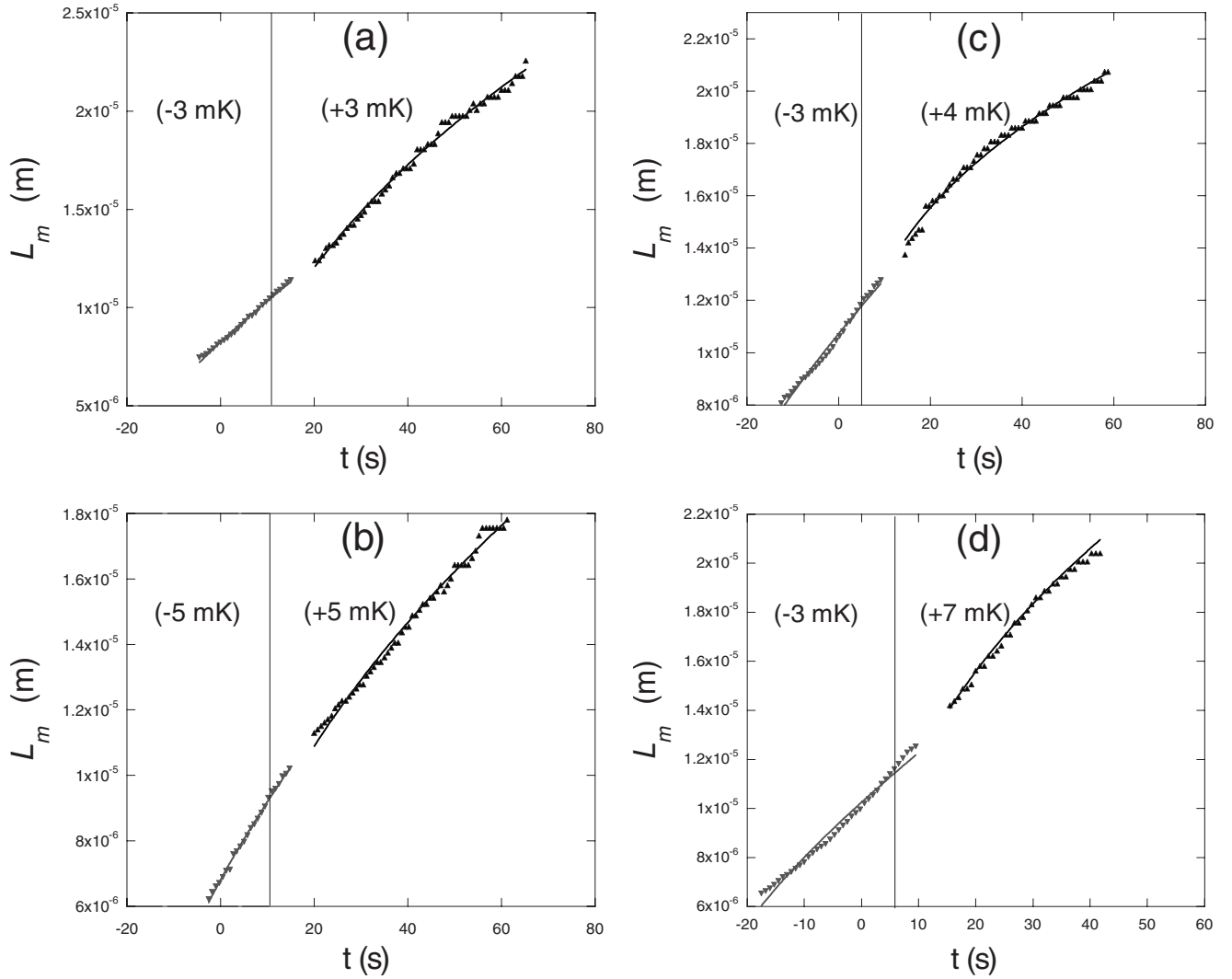
FIG. 3. Evolution of the typical domain length scale for two double-quench experiments: (a) $(+3,-3,+3)$ mK performed at time $t_{\mathrm{I}}=-40$ s, (b) $(+5,-5,+5)$ mK performed at time $t_{\mathrm{I}}=-40$ s, (c) $(+3,-3,+4)$ mK performed at time $t_{\mathrm{I}}=-40$ s, (d) $(+3,-3,+7)$ mK performed at time $t_{\mathrm{I}}=-40$ s. $T<T_c$ (gray triangles downward): fit to Eq. (9) (gray curve). $T>T_c$ (black triangles upward): fit to Eq. (17) (black curve). The vertical line corresponds to time t_2 (see text).

B. Evolution above T_c

When the temperature is set back to T_i (t larger than t_{II}), the peaked shapes of the structure factors around a k_m value are preserved for some time, as well as the decrease of k_m with time. This behavior means that the domains are still growing. As diffusion now acts to dissolve the domains, the origin of the coarsening can only be found in the persistence of capillary flows and then shows the preservation of surface tension. However, the surface tension must decrease with time since diffusion thickens the domain interfaces and lowers the concentration of the phases. When plotted together, one can observe a modification in the behavior of $L_m(t)$ between the two-phase and one-phase regions. Similarly, the scaling of the structure factor $[F(x)\sim \mathrm{const}]$ is also preserved for about 20 s [Fig. 2(b)], and a progressive breaking of scaling occurs with time. This phenomenon is very progressive and corresponds also to the modification of the L_m evolution [Fig. 3].

In agreement with the expectation that the coarsening in the monophasic region is due to a transient surface tension, we assume the L_m evolution above T_c, L_m^+, to be similar to Eq. (9), but without the first diffusive term as discussed above,

$$L_m^+ = L_0 + b\left(\frac{\sigma^+(t)}{\eta}\right)(t-t_2), \tag{10}$$

where $\sigma^+(t)$ represents the transient surface tension that we analyze below and t_2 is the time when the temperature in the sample returns to T_i. In the following, we propose a model that fits the data of the evolution of $\sigma^+(t)$ (Figs. 3 and 4). L_0 is the pattern wavelength reached at time t_2. Note that the b value has no reason to be equal to the previous value of 8.70×10^{-2}, which has been determined in the two-phase region.
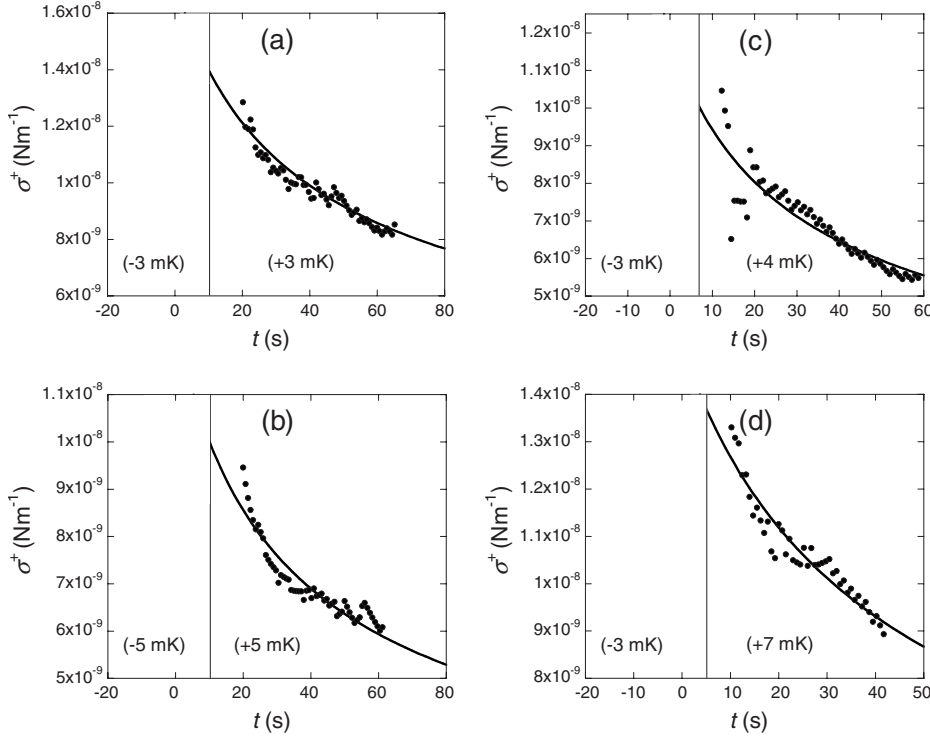
FIG. 4. Corresponding decrease of the surface tension with time for the four evolutions depicted in Figs. 3(a)–3(d), respectively. Full line: fit to Eq. (18).

C. Surface-tension evolution

The surface-tension evolution can be calculated within an approach derived from statistical mechanics adapted to a planar interface [4]. The surface tension is derived from the expression of the pressure tensor given by Irving and Kirkwood [28] within an approximation of small concentration gradients. The surface tension can then be written as [4]

$$\sigma = c \int \left(\frac{d\Phi}{dz} \right)^2 dz, \qquad (11)$$

where $c = n^2[c_{11} + c_{22} - c_{12}]$, with n as the total density of the mixture and

$$c_{\alpha\beta} = \left(\frac{2\pi}{15} \right) \int s^3 \left(\frac{du_{\alpha\beta}}{ds} \right)(s) g_{\alpha\beta}(s) d^3s, \qquad (12)$$

where $u_{\alpha\beta}(s)$ is the pair potential between particles of components α and β separated by s, and $g_{\alpha\beta}(s)$, the pair-correlation function. $\Phi(z)$ corresponds to the mole fraction profile across the interface and is given by

$$\Phi(z) = 1/2[(\Phi_1 + \Phi_2) - (\Phi_1 - \Phi_2)f(z)], \qquad (13)$$

where $\Phi_{1,2}$ are the molar fraction of phases 1 and 2, respectively, and $f(z)$ a function approaching ± 1 when z, the normal coordinate to the interface, approaches $\pm\infty$. An excellent approximation is to consider the interface profile as arising from a time average of capillary waves since this profile was successfully compared to reflectivity measurements [29,30]: $f(z) = \mathrm{erf}(\sqrt{\pi}z/l_i)$. The interface thickness l_i at $T < T_c$ was determined to be $l_i \approx 16\xi^-$ in order to reproduce experimental data. In the framework of local equilibrium, we make the assumption that the time evolution at $T_i \gtrsim T_c$ is described by a widening of the interface thickness $l(t)$ by diffusion, the

concentration profile keeping the error function dependence $f(z) = \mathrm{erf}[\sqrt{\pi}z/l_i(t)]$. The profile now verifies a diffusion equation with a diffusion coefficient $D^+ = k_B T/6\pi\eta\xi^+(T_i)$,

$$\dot{f} = D^+ \partial^2 f/\partial z^2, \qquad (14)$$

and one finds

$$l^2(t) = 4\pi D^+ t + l_i^2. \qquad (15)$$

Note that this diffusion equation is an approximation since close to the critical point the real dynamical equation should stem from a time-dependent Ginzburg-Landau equation derived from the free energy. However, its derivation is quite beyond the scope of the present paper. Then, the surface-tension evolution for $T_i \gtrsim T_c$, $\sigma^+(t)$, can be calculated, thanks to Eq. (11), with t becoming $t - t_2$,

$$\sigma^+(t) = \frac{\sigma}{\sqrt{1 + \dfrac{4\pi D^+}{l_i^2}(t - t_2)}}. \qquad (16)$$

The prefactor of the surface tension, σ, is identified with the surface tension at the temperature reached before quenching up, expected to be close to σ_{fit} reached below T_c and l_i is the interfacial thickness at the same temperature.

Equation (16) is only valid for $t > t_2$ and, once introduced in Eq. (10), gives a proper fitting function for L_m,

$$L_m = L_0 + b\left(\frac{\sigma}{\eta} \right) \frac{t - t_2}{\sqrt{1 + \dfrac{4\pi D^+}{l_i^2}(t - t_2)}}. \qquad (17)$$

Note that, contrary to l_i, L_m is still a growing function of time since the latter quantity obeys a hydrodynamic equation and

not a diffusive one as l_i. Of course, L_m will lose its one dimension meaning at times longer than the ones under study, when concentration profiles mix with each other. Here, l_i corresponds to the thickness of the domain interfaces at time t_2 and should be compared to $16\xi^-$. The best fits (Fig. 3) are found with an imposed t_2 between 5 and 10 s (in agreement with what is known about thermal evolution for an upward quench) and L_0, σ, and l_i left free. The values are reported in Table I (lower row). For these fits, we decided to set $b = 8.7 \times 10^{-2}$ determined for the two-phase region. As noted above, the uncertainty in b prevents us from drawing any precise conclusions from the obtained values of σ_{fit}. We note that they are slightly higher than the determined σ_{fit} values in the two-phase region which means that b could be somewhat higher in the one-phase region. About l_i, the values are somewhat larger but fully compatible with the expected values at the one-phase temperatures. This slight disagreement can be due to two distinct factors. The first one concerns the oversimplifications made in the modeling of the surface-tension evolution. The second one—probably the most important one—is the widening of $l(t)$ between t_{II} and t_2 since the upward quench takes some time to be completed. However, the consistency of the fit parameters validates our procedure, which is indeed accurately controlled in time and temperature and amenable to a quantitative analysis.

In order to make apparent the evolution of the surface tension during remixing, we have plotted in Figs. 4 the transient surface tension as deduced from Eq. (10); it fits to

$$\sigma^+(t) = \frac{\sigma_{fit}}{\sqrt{1 + \dfrac{4\pi D^+}{l_{i,fit}^2}(t - t_2)}}. \tag{18}$$

The data show clearly the decrease of the surface tension with time. Comparable evolutions were already reported, and it is interesting to compare these previous findings with the present results. In Ref. [10], the same IW mixture was investigated by measuring the surface tension by the spinning drop method. The time evolution of $\sigma/\Delta\rho$ in the one-phase region, where $\Delta\rho$ is the density difference between the two miscible phases, was found to follow a nonmonotonous decrease, exhibiting a local maximum at some time. This peculiar behavior was attributed to the coupled evolution of the surface tension and the density difference. In Ref. [13], surface tensions of several 10^{-7} N/m were found, corresponding to a much larger distance to the critical point than in our experiment where $\sigma \approx 10^{-9}$ N/m. Fits of the Ref. [13] results to a diffusion equation lead to diffusion coefficient several orders of magnitude lower than expected at those temperatures. In Ref. [14], the nonequilibrium bulk fluctuations were taken into account for properly isolating the interface scattering signal. Surface-tension variations were detected at a distance from the critical point even larger than in Ref. [13]. The reported variations span a large range between 3×10^{-5} and 3×10^{-7} N/m but no quantitative analysis was reported. In the latter two cases, because large temperature steps were performed between the two-phase and the one-phase regions, a large uncertainty is likely to reside in the time where the system becomes monophasic. In contrast, since our experiment involves only minute temperature steps, the determination of this latter time is in agreement with thermal behaviors. This explains why our experiments can be analyzed within the local equilibrium hypothesis, which makes quantitative the diffusive analysis that we have presented.

V. CONCLUSION

This study was performed with a partially miscible density matched binary liquid in the close vicinity of its critical point where dynamics is largely slowed down. It unambiguously shows the existence of a transient nonzero surface tension between miscible fluids. The surface-tension relaxation can be convincingly represented by a simple model of interface diffusion and local equilibrium. It then follows that the use of a dynamic surface-tension term in the fluid mechanics of miscible phases is fully justified.

ACKNOWLEDGMENTS

[1] P. Petijeans, C. R. Acad. Sci., Paris, t 325, Ser. II **86**, 587 (1996).

[2] R. J. Hunter, *Foundations of Colloid Science* (Oxford University Press, New York, 1987), pp. 234–237.

[3] J. S. Rowlinson and B. Widom, *Molecular Theory of Capillarity* (Oxford University Press, Oxford, 1982).

[4] H. T. Davis, *Numerical Simulation and Oil Recovery* (Springer-Verlag, Berlin, 1988), pp. 105–110.

[5] D. Korteweg, Arch. Néerl. Sci. Ex. Nat., Série II **6**, 1 (1901).

[6] X. F. Liu, E. George, W. G. Bo, and J. Glimm, Phys. Rev. E **73**, 056301 (2006).

[7] C.-Y. Chen, C.-W. Huang, H. Gadelha, and J. A. Miranda, Phys. Rev. E **78**, 016306 (2008).

[8] J. E. Mungall, Phys. Rev. Lett. **73**, 288 (1994).

[9] B. Zoltowski, Y. Chekanov, J. Masere, J. A. Pojman, and V. Volpert, Langmuir **23**, 5522 (2007).

[10] J. A. Pojman, C. Whitmore, M. L. T. Liveri, R. Lombardo, J. Marszalek, R. Parker, and B. Zoltowski, Langmuir **22**, 2569 (2006).

[11] G. Viner and J. Pojman, Opt. Lasers Eng. **46**, 893 (2008).

[12] N. Bessonov, J. A. Pojman, G. Viner, V. Volpert, and B. Zoltowski, Math. Model. Nat. Phenom. **3**, 108 (2008).

[13] S. E. May and J. V. Maher, Phys. Rev. Lett. **67**, 2013 (1991).

[14] P. Cicuta, A. Vailati, and M. Giglio, Appl. Opt. **40**, 4140 (2001).

[15] A. Onuki, *Phase Transition Dynamics* (Cambridge University

Press, Cambridge, 2002), pp. 421–425.

[16] E. D. Siggia, Phys. Rev. A **20**, 595 (1979).

[17] P. Guenoun, R. Gastaud, F. Perrot, and D. Beysens, Phys. Rev. A **36**, 4876 (1987).

[18] A. Kumar, H. R. Krishnamurthy, and E. S. R. Gopal, Phys. Rep. **98**, 57 (1983).

[19] F. Kammoun, J. P. Astruc, D. Beysens, P. Hede, and P. Guenoun, Rev. Sci. Instrum. **63**, 3659 (1992).

[20] D. Beysens and A. Bourgou, Phys. Rev. A **19**, 2407 (1979).

[21] A. Thill, S. Désert, and M. Delsanti, Eur. Phys. J.: Appl. Phys. **17**, 201 (2002).

[22] D. Beysens, A. Bourgou, and G. Paladin, Phys. Rev. A **30**, 2686 (1984).

[23] V. S. Nikolayev, D. Beysens, and P. Guenoun, Phys. Rev. Lett. **76**, 3144 (1996).

[24] H. Furukawa, Adv. Phys. **34**, 703 (1985).

[25] M. R. Moldover, Phys. Rev. A **31**, 1022 (1985).

[26] S. C. Greer, Phys. Rev. A **14**, 1770 (1976).

[27] D. Beysens, Microgravity Q. **5**, 34 (1995).

[28] J. H. Irving and J. G. Kirkwood, J. Chem. Phys. **18**, 817 (1950).

[29] D. Beysens and M. Robert, J. Chem. Phys. **87**, 3056 (1987).; **93**, 6911 (1990).

[30] F. P. Buff, R. A. Lovett, and F. H. Stillinger, Phys. Rev. Lett. **15**, 621 (1965).